Proteins and Ions Compete for Membrane Interaction: the case of Lactadherin

A. M. De Lio, D. Paul, R. Jain, J. H. Morrissey*, T. V. Pogorelov*

Biophysical Letters

ABSTRACT

Charged molecular species, such as ions, play a vital role in the life of the cell. In particular, divalent calcium ions (Ca^{2+}) are critical for activating cellular membranes. Interactions between Ca^{2+} and anionic phosphatidylserine (PS) lipids result in structural changes of the plasma membrane and are vital for many signaling pathways, such as the tightly regulated blood coagulation cascade. Upon cell damage, PS lipids are externalized to the outer leaflet, where they are not only exposed to Ca^{2+}, but also to proteins. Lactadherin is a glycoprotein, important for cell-adhesion, that competes with Ca^{2+} and blood clotting proteins in binding PS lipids, leading to a negative impact on key steps in the coagulation cascade. While a number of experimental studies have been performed on lactadherin's C2 domain's (LactC2) binding affinity for PS molecules, an atomistic description of LactC2 interactions with PS lipids in the plasma membrane is lacking. We performed extensive all-atom sampling and experimental characterization of LactC2-membrane interactions in the presence and absence of Ca^{2+} and characterized PS-Ca^{2+} and PS-LactC2 interactions to guide our understanding of how these interactions initiate and impede blood coagulation, respectively. We captured spontaneously formed long-lived PS-Ca^{2+} and PS-LactC2 complexes and revealed that the protein sidechains involved in PS-LactC2 interactions appear to be affected by the presence of Ca^{2+}. The insertion of LactC2 into the lipid bilayer appears to be dependent on the presence of Ca^{2+}. Characterizing the competing interactions between Ca^{2+} and lactadherin with PS lipids can lead to a greater understanding of the activation and regulation of the blood coagulation cascade and of the basis of charged species competition for lipid membrane.

STATEMENT OF SIGNIFICANCE

Lactadherin plays an important role in several cellular processes. Many of these processes involve lactadherin interacting with the lipids of the cell plasma membrane. One such process is the blood coagulation cascade. Lactadherin acts as an anticoagulant and contributes to a number of health issues. Understanding the interactions that drive lactadherin's anticoagulant properties can lead to potential targets for treatments.

INTRODUCTION

Lactadherin, originally identified as a milkfat globule glycoprotein, has been shown to bind to the plasma membrane via interactions with phosphatidyl-L-serine (PS) lipids. Lactadherin has been found to participate in a number of cellular processes including bilayer stabilization (1), mediating apoptotic clearance of lymphocytes (2, 3) and epithelial cells (4), and clearing amyloid ß-peptide, a key component of Alzheimer disease. Lactadherin has also been found to help regulate the blood coagulation cascade by acting as an anticoagulant (5).

Bovine lactadherin, studied here, is comprised of four domains, two epidermal growth factor domains and two discoidin domains (EGF1-EGF2-C1-C2). The C2 domain of lactadherin (LactC2) has been found to be the primary location of PS binding (6).

LactC2 functions as an anticoagulant by blocking PS binding sites from use by coagulation factors such as factor VIII, the prothrombinase complex, and the factor VIIa-tissue factor complex, many of which are mediated by divalent calcium ion (Ca^{2+})-PS interactions. Unlike many of the components of the coagulation cascade, LactC2 does not require Ca^{2+} to mediate interactions with the membrane surface (5). This suggests that a direct competition could exist between LactC2 and Ca^{2+} for PS binding sites.

The LactC2 domain is structurally similar to the C domains in some blood coagulation factors, such as factor V (fV-C2) and factor VIII (fVIII-C2). LactC2, fV-C2, and fVIII-C2 are structurally similar and all contain long loops, here referred to as Spikes. These Spikes contain water-exposed hydrophobic residues. Site-directed mutagenesis of these hydrophobic residues has highlighted their importance in the functionality of lactadherin. It has been hypothesized that the hydrophobic residues of these Spikes insert into the membrane (7), but detailed studies are lacking. Characterizing the types of interactions that take place at the membrane surface can aid in our understanding of lactadherin's role as a coagulation cascade regulator and how charged moieties affect and shape the plasma membrane.

Here we utilize all-atom molecular dynamics (MD) simulations and binding studies to capture LactC2 membrane insertion and the competition between LactC2 and Ca^{2+} for membrane binding sites. We also characterize the key charged species-lipid interactions both in the presence and absence of Ca^{2+}.

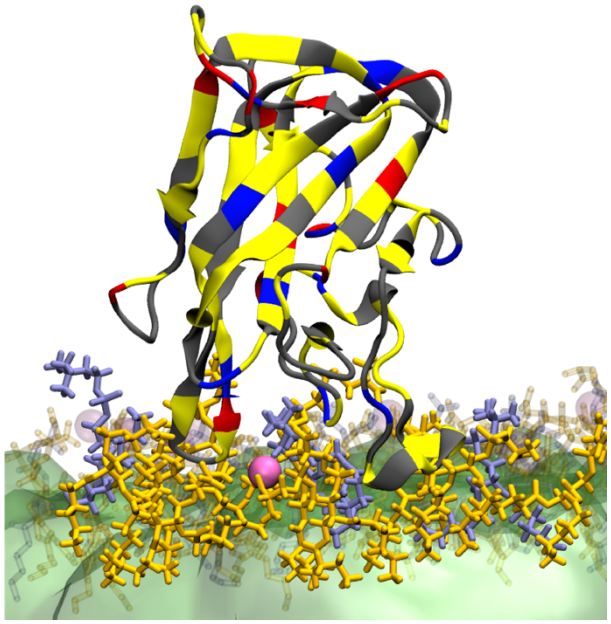

Figure 1. Snapshot of LactC2 inserted in the short-tail PS (orange)/PC (gray-blue) HMMM plasma membrane with dichloroethane (DCLE) (green) solvent in the presence of Ca^{2+} (pink). Transparent lipids and Ca^{2+} are farther than 3Å from any LactC2 residues. Residues colored by type: polar (gray), non-polar (yellow), basic (blue), and acidic (red).

RESULTS & DISCUSSION

To investigate the dominating types of interactions between LactC2 and the plasma membrane, it was necessary to capture these interactions at atomic resolution. Crystal structure analysis of the LactC2 domain

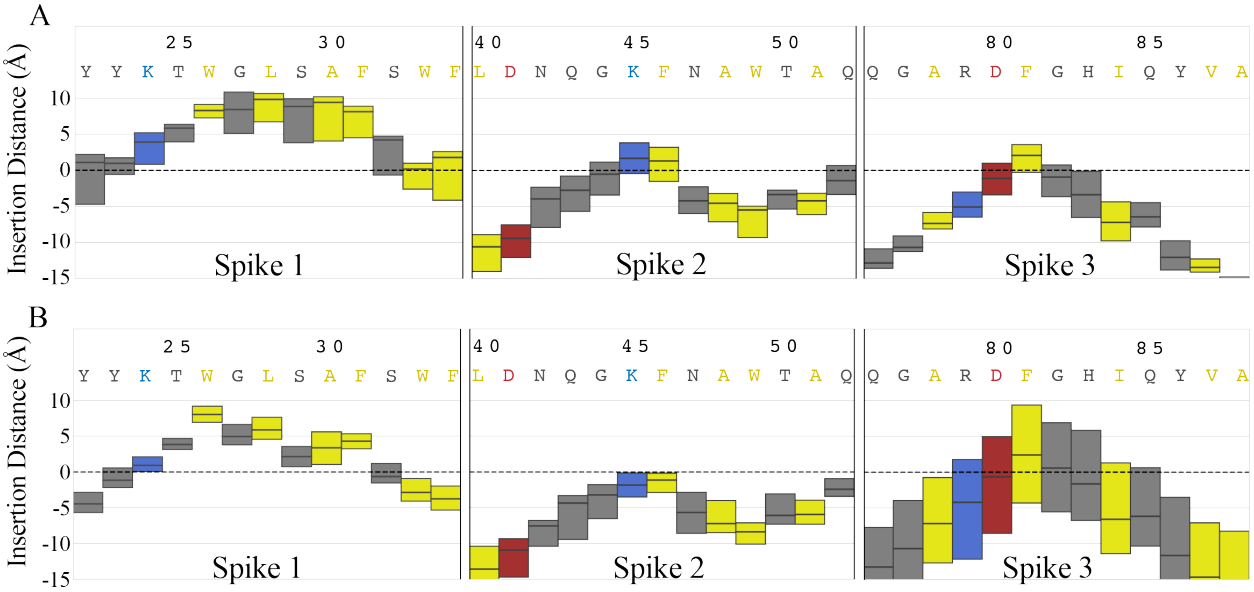

Figure 2. Average insertion of Spikes 1, 2, 3 of LactC2 into membrane. Insertion distance between the lipid phosphorous atom plane (dashed line) and the center of mass of the residues over the last 50 ns of simulations. Residue insertion depths are positive inside the membrane and are color coded by residue type: polar (gray), non-polar (yellow), basic (blue), and acidic (red). (A) Insertion of LactC2 residues in the replicas containing Ca^{2+}. (B) Insertion of LactC2 residues in the replicas containing no ions.

suggests that Spikes 1, 2, and 3 can insert into the plasma membrane as they contain a number of hydrophobic residues (7). To capture the insertion two systems were assembled, one in the presence of Ca^{2+} and one in the absence of Ca^{2+} (Figure S1). We performed extensive all-atom equilibrium MD simulations using the highly-mobile membrane mimetic (HMMM) (8–10) of both systems and observed spontaneous reproducible insertions of LactC2 into the lipid bilayer (Figure 1). After 250 ns of expedited HMMM simulations, the short-tail lipids were extended to full representations and modeled for additional 50 ns which were analyzed to measure the depth of insertion of LactC2's Spikes and to characterize the types of interactions happening at the surface of the membrane between charged LactC2 residues and lipid headgroups.

We observed consistent insertion of Spikes 1 and 3 into the bilayer in the presence (Figures 2A and S2), and absence (Figures 2B and S3) of Ca^{2+}. The height of the bars in Figure 2, which corresponds to the 25-75% quartiles, indicate the average amount of up-and-down motion experienced by the Spikes during the analyzed trajectories. The insertion data offers a number of insightful details about how the insertion of LactC2 is affected by the presence of Ca^{2+}. Firstly, the degree of vertical motion experienced by LactC2 is consistent regardless of the presence of Ca^{2+} (Figures S2 and S3). In the instance of a direct interaction between Ca^{2+} and the D80 residue of LactC2, the motion is even less varied, suggesting an anchoring effect for the region - Spike 3 (Figure S2B). This direct LactC2-Ca^{2+} interaction was not anticipated as LactC2 does not functionally require Ca^{2+} (5), however based on the electrostatic properties of D80 and Ca^{2+}, it is not surprising.

We also observe that the depth of insertion of the Spikes is greater in the presence of Ca^{2+} (Figures 2, S2, S3). The charged residues K24 and K45 stop just at the surface of the membrane in the absence of Ca^{2+} but can insert up to 6 Å in the presence of Ca^{2+}. The ability of the charged

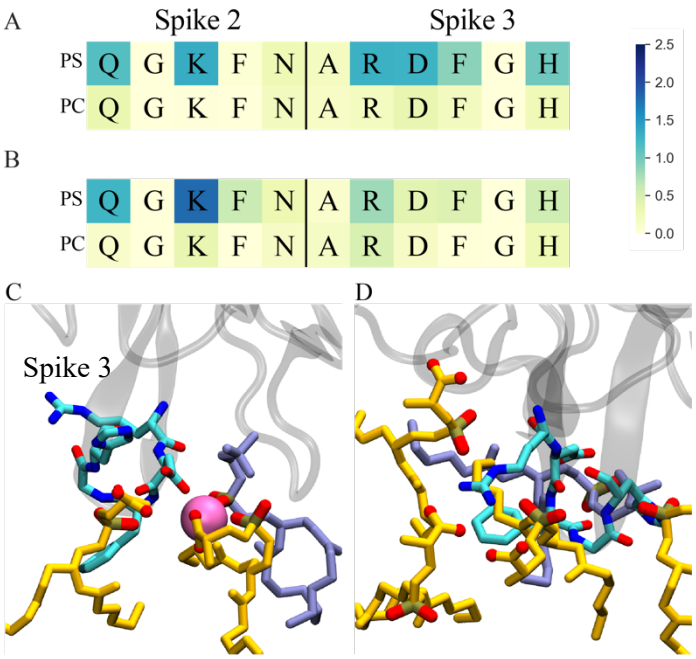

Figure 3. Mean contact number between the residues in Spikes 2 & 3 of LactC2 and individual PS and PC molecules in the membrane (A) in the presence of Ca^{2+} and (B) in the absence of Ca^{2+}. Snapshots of Spike 3 residue interactions (C) in the presence of Ca^{2+} and (D) in the absence of Ca^{2+}. Residues are colored by atom name. PS (orange), PC (gray-blue) show headgroup carboxy oxygens and phosphate groups colored by atom type.

Spike residues to insert into the bilayer, rather than just sit on top, subsequently allows the hydrophobic residues of the Spikes to insert more deeply into the hydrophobic core of the bilayer and anchor the domain. We took a closer look at the number of PS and PC contacts the Spike residues encountered both in the presence and absence of Ca^{2+} (Figure 3A and B). In both systems we see consistent interactions between LactC2 and the membrane lipids. We also observe that, in both systems, LactC2 has a larger number of contacts with PS than with phosphatidylcholine (PC). This is consistent with the idea that LactC2 preferentially binds PS and does not bind PC (6, 11).

As stated previously, we did observe one instance of a LactC2-Ca^{2+} interaction which demonstrates that LactC2 residues can also interact with Ca^{2+} moieties via sidechain carboxy oxygens (Figure 3C). In the absence of Ca^{2+}, positively charged residues, such as K45 in Spike 2, have more interactions with PS lipids (Figure 3B). Figure 3D shows a snapshot of the interactions between R79 and nearby PS lipids. In similarity to the interactions between Ca^{2+} and PS lipids (12), we find both the carboxy oxygens and phosphate oxygens of PS interact with R79.

We performed surface plasmon resonance (SPR) studies of lactadherin on PS/PC nanodiscs to characterize the effect of increased insertion depth of LactC2 into the membrane surface and to determine whether the presence of Ca^{2+} moieties affects the binding affinity of lactadherin to the membrane surface. To our knowledge, this is the first report on the binding affinity of lactadherin using nanodiscs as the membrane model and we find that the binding affinity in the absence of Ca^{2+} is 296.2 ± 82.84 (nM), which is in agreement with previously reported literature (13). In order to more accurately model a physiologically relevant system, we also measured the binding affinity of lactadherin in the presence of Ca^{2+}; which was measured to be 283.0 ± 66.47 (nM). These values suggest that there is no change in the binding affinity of lactadherin to the membrane model in the presence and absence of Ca^{2+} (Figure 4A). Since LactC2 binds PS in a Ca^{2+}-independent manner (5), we expected to observe similar binding affinities in both systems. This is also in agreement with our computational observation that LactC2-PS interactions occur regardless of the presence or absence of Ca^{2+} (Figure 3A and 3B).

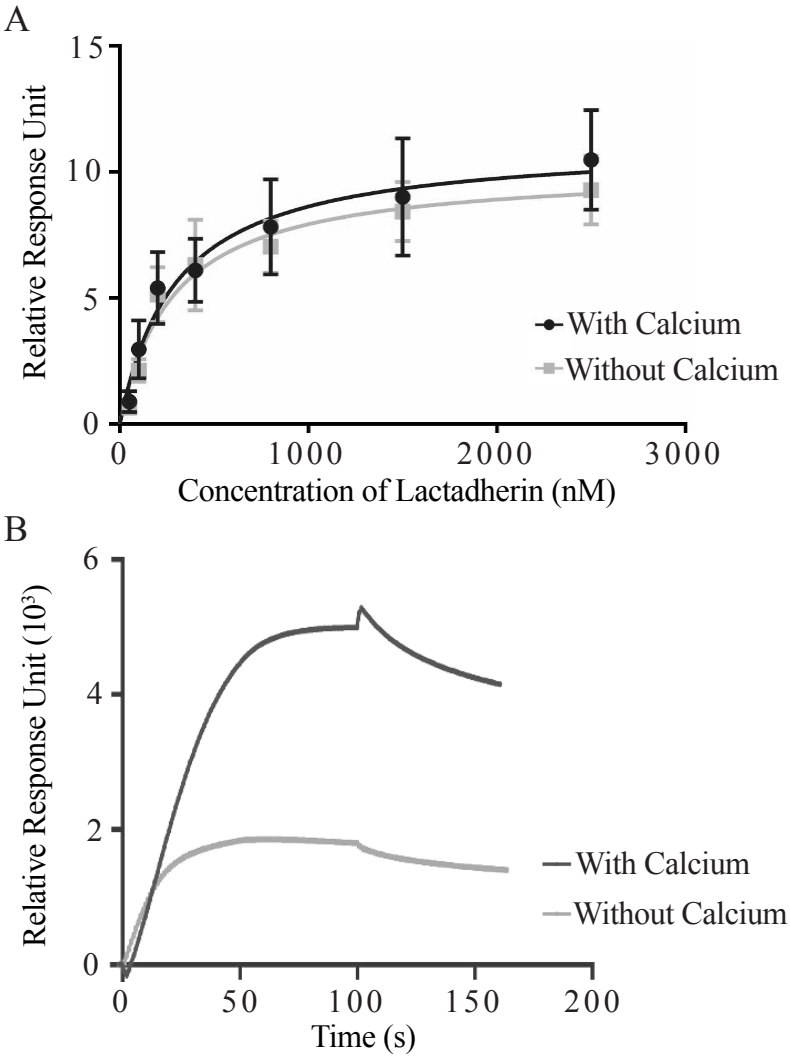

Figure 4. Experimental studies on lactadherin interaction with nanodiscs. (A) Comparison of binding affinities of lactadherin in the presence of (blue) and absence of (red) Ca^{2+}. (B) Association times of lactadherin in the presence of (red) and absence of (blue) Ca^{2+}.

We hypothesized that Ca^{2+} and the charged residues of the Spikes would compete for the charged lipid headgroup binding sites of the membrane. While we did not observe any exchange of PS binding sites between Ca^{2+} and LactC2 residues in our simulations due to time scale limitations, we used SPR to determine if the association time of lactadherin to the membrane was affected by the presence of Ca^{2+} (Figure 3B). We observed an increase in the association time of lactadherin to the membrane in the presence of Ca^{2+} versus in the absence of Ca^{2+}. This may indicate a competition of lactadherin and Ca^{2+} for PS binding sites.

To determine the effect the Ca^{2+} has on the stability of the LactC2 secondary structure, we performed network analysis on LactC2 domain in both systems (Figure S4). In the absence of Ca^{2+} the backbone interactions of the residues in Spike 3 are strong, indicated by thick linking lines (Figure S4B). In the presence of Ca^{2+} we observe the same backbone interactions are now weaker (Figure S4A). This is an indication that the LactC2-Ca^{2+} interactions destabilize the structure of Spike 3.

CONCLUSIONS

We have captured reproducible spontaneous insertion of the LactC2 domain into the lipid bilayer. While the hydrophobic residues of the Spikes may be integral for lactadherin function, the charge-driven interactions between the lipid headgroups and LactC2 or Ca^{2+} determine insertion depth, the mobility of LactC2 once bound to the membrane, and the stability of the backbone interactions. Binding studies of lactadherin to nanodiscs demonstrated that its binding affinity to the membrane is independent of the presence of Ca^{2+} but that the association time to the membrane surface is directly affected by Ca^{2+}. These results reveal a direct competition between lactadherin and Ca^{2+} for binding sites on the membrane surface and will guide future studies to characterize

the mechanism lactadherin employs as an anticoagulant and regulator of the blood coagulation cascade and the roles charged species play in critical protein-lipid interactions.

AUTHOR CONTRIBUTIONS

A.M.D. performed MD simulations on the systems containing no Ca^{2+} moieties. R.J. performed MD simulations on Ca^{2+} containing replicas. A.M.D. performed all analysis of MD simulations including insertions depth, contact number, and network analysis. T.V.P. supervised the entirety of the computational studies. D.P. performed all binding studies and completed all the analysis corresponding to those studies. J.H.M. supervised the binding studies.

ACKNOWLEDGEMENTS

The authors are grateful for support from a National Institutes of Health Transformative Research Award (R01 GM123455) and NHLBI grant R35 HL135823. T.V.P. acknowledges support from the Department of Chemistry, the School of Chemical Sciences, and the Office of the Vice-Chancellor for Research (RSOCR Award 4703) at University of Illinois at Urbana-Champaign and computational resources from the Texas Advanced Computing Center (TACC) at the University of Texas at Austin made available from the Extreme Science and Engineering Discovery Environment (XSEDE) Grant TG-MCB130112, which is supported by National Science Foundation Grant ACI-1053575. A.M.D. is supported by a postdoctoral fellowship from the National Center for Supercomputing Resource and Cyprus Institute.

SUPPORTING CITATIONS

References (14-37) appear in the Supporting Material.

REFERENCES

1. Butler, J.E., D.J. Pringnitz, C.L. Martens, and N. Crouch. 1980. Bovine-Associated Mucoprotein: I. Distribution Among Adult and Fetal Bovine Tissues and Body Fluids. Differentiation. 17: 31–40.
2. Hanayama, R., M. Tanaka, K. Miwa, A. Shinohara, A. Iwamatsu, and S. Nagata. 2002. Identification of a factor that links apoptotic cells to phagocytes. Nature. 417: 182–187.
3. Hanayama, R., M. Tanaka, K. Miyasaka, K. Aozasa, M. Koike, Y. Uchiyama, and S. Nagata. 2004. Autoimmune disease and impaired uptake of apoptotic cells in MFG-E8-deficient mice. Science (80-.). 304: 1147–1150.
4. Hanayama, R., and S. Nagata. 2005. Impaired involution of mammary glands in the absence of milk fat globule EGF factor 8. Proc. Natl. Acad. Sci. U. S. A. 102: 16886–16891.
5. Shi, J., and G.E. Gilbert. 2003. Lactadherin inhibits enzyme complexes of blood coagulation by competing for phospholipid-binding sites. Blood. 101: 2628–2636.
6. Andersen, M.H., H. Graversen, S.N. Fedosov, T.E. Petersen, and J.T. Rasmussen. 2000. Functional analyses of two cellular binding domains of bovine lactadherin. Biochemistry. 39: 6200–6206.
7. Shao, C., V.A. Novakovic, J.F. Head, B.A. Seaton, and G.E. Gilbert. 2008. Crystal structure of lactadherin C2 domain at 1.7 A° resolution with mutational and computational analyses of its membrane-binding motif. J. Biol. Chem. 283: 7230–7241.
8. Vermaas, J. V., J.L. Baylon, M.J. Arcario, M.P. Muller, Z. Wu, T. V. Pogorelov, and E.

Tajkhorshid. 2015. Efficient Exploration of Membrane-Associated Phenomena at Atomic Resolution. J. Membr. Biol. 248: 563–582.
9. Ohkubo, Y.Z., T. V. Pogorelov, M.J. Arcario, G.A. Christensen, and E. Tajkhorshid. 2012. Accelerating membrane insertion of peripheral proteins with a novel membrane mimetic model. Biophys. J. 102: 2130–2139.
10. Pogorelov, T. V., J. V. Vermaas, M.J. Arcario, and E. Tajkhorshid. 2014. Partitioning of amino acids into a model membrane: Capturing the interface. J. Phys. Chem. B. 118: 1481–1492.
11. Andersen, M.H., L. Berglund, J.T. Rasmussen, and T.E. Petersen. 1997. Bovine PAS-6/7 binds α(v)β5 integrin and anionic phospholipids through two domains. Biochemistry. 36: 5441–5446.
12. Hallock, M.J., A. Greenwood, Y. Wang, J.H. Morrissey, E. Tajkhorshid, C. Rienstra, and T. V. Pogorelov. 2017. Calcium-Induced Sculpturing of the Plasma Membrane: Lipid Microclusters Cast by Anionic Lipids. Biophys. J. 112: 467a-468a.
13. Del Vecchio, K., and R. V. Stahelin. 2018. Investigation of the phosphatidylserine binding properties of the lipid biosensor, Lactadherin C2 (LactC2), in different membrane environments. J. Bioenerg. Biomembr. 50: 1–10.
14. Pande, A.H., S. Qin, and S.A. Tatulian. 2005. Membrane fluidity is a key modulator of membrane binding, insertion, and activity of 5-lipoxygenase. Biophys. J. 88: 4084–4094.
15. Wimley, W.C., T.P. Creamer, and S.H. White. 1996. Solvation energies of amino acid side chains and backbone in a family of host - Guest pentapeptides. Biochemistry. 35: 5109–5124.
16. MacCallum, J.L., W.F. Drew Bennett, and D. Peter Tieleman. 2008. Distribution of amino acids in a lipid bilayer from computer simulations. Biophys. J. 94: 3393–3404.
17. Jo, S., T. Kim, V.G. Iyer, and W. Im. 2008. CHARMM-GUI: A Web-Based Graphical User Interface for CHARMM. J. Comput. Chem. 29: 1859–1865.
18. Brooks, B.R., C.L. Brooks III, A.D. Mackerell Jr., L. Nilsson, R.J. Petrella, B. Roux, Y. Won, G. Archontis, C. Bartels, S. Boresch, A. Caflisch, L. Caves, Q. Cui, A.R. Dinner, M. Feig, S. Fischer, J. Gao, M. Hodoscek, W. Im, K. Kuczera, T. Lazaridis, J. Ma, V. Ovchinnikov, E. Paci, R.W. Pastor, C.B. Post, J.Z. Pu, M. Schaefer, B. Tidor, R.M. Venable, H.L. Woodcock, X. Wu, W. Yang, D.M. York, and M. Karplus. 2009. CHARMM: The Biomolecular Simulation Program. J. Comput. Chem. 30: 1545–1614.
19. Lee, J., X. Cheng, J.M. Swails, M.S. Yeom, P.K. Eastman, J.A. Lemkul, S. Wei, J. Buckner, J.C. Jeong, Y. Qi, S. Jo, V.S. Pande, D.A. Case, C.L. Brooks, A.D. MacKerell, J.B. Klauda, and W. Im. 2016. CHARMM-GUI Input Generator for NAMD, GROMACS, AMBER, OpenMM, and CHARMM/OpenMM Simulations Using the CHARMM36 Additive Force Field. J. Chem. Theory Comput. 12: 405–413.
20. Qi, Y., X. Cheng, J. Lee, J. V. Vermaas, T. V. Pogorelov, E. Tajkhorshid, S. Park, J.B. Klauda, and W. Im. 2015. CHARMM-GUI HMMM Builder for Membrane Simulations with the Highly Mobile Membrane-Mimetic Model. Biophys. J. 109: 2012–2022.
21. Phillips, J.C., R. Braun, W. Wang, J. Gumbart, E. Tajkhorshid, E. Villa, C. Chipot, R.D. Skeel, L. Kalé, and K. Schulten. 2005. Scalable molecular dynamics with NAMD. J. Comput. Chem. 26: 1781–1802.
22. Klauda, J.B., R.M. Venable, J.A. Freites, J.W. O'Connor, D.J. Tobias, C. Mondragon-Ramirez, I. Vorobyov, A.D. Mackerell Jr., R.W. Pastor, and J.W.O. Connor. 2011. Update of the CHARMM all-atom additive force field for lipids. J. Phys. Chem. B. 114: 7830–

7843.
23. Vanommeslaeghe, K., E. Hatcher, C. Acharya, S. Kundu, S. Zhong, J. Shim, E. Darian, O. Guvench, P. Lopes, I. Vorobyov, and A.D. MacKerell Jr. 2010. CHARMM General Force Field (CGenFF): A Force Field for Drug-like Molecules Compatible with the CHARMM All-Atom Additive Biological Force Fields. J. Comput. Chem. 31: 671–690.
24. Jorgensen, W.L., J. Chandrasekhar, J.D. Madura, R.W. Impey, and M.L. Klein. 1983. Comparison of simple potential functions for simulating liquid water. J. Chem. Phys. 79: 926–935.
25. 2018. Python 3.7.7 documentation. .
26. Hunter, J.D. 2007. Matplotlib: A 2D graphics environment. Comput. Sci. Eng. 9: 99–104.
27. Waskom, M., O. Botvinnik, P. Hobson, J.B. Cole, Y. Halchenko, S. Hoyer, A. Miles, T. Augspurger, T. Yarkoni, T. Megies, L.P. Coelho, D. Wehner, Cynddl, E. Ziegler, Diego0020, Y. V. Zaytsev, T. Hoppe, S. Seabold, P. Cloud, M. Koskinen, K. Meyer, A. Qalieh, and D. Allan. 2014. seaborn: v0.5.0. .
28. McKinney, W. 2010. Data Structures for Statistical Computing in Python. : 51–56.
29. Van Der Walt, S., S.C. Colbert, and G. Varoquaux. 2011. The NumPy array: A structure for efficient numerical computation. Comput. Sci. Eng. 13: 22–30.
30. Gowers, R., M. Linke, J. Barnoud, T. Reddy, M. Melo, S. Seyler, J. Domański, D. Dotson, S. Buchoux, I. Kenney, and O. Beckstein. 2016. MDAnalysis: A Python Package for the Rapid Analysis of Molecular Dynamics Simulations. Proc. 15th Python Sci. Conf. : 98–105.
31. Michaud-Agrawal, N., E.J. Denning, T.B. Woolf, and O. Beckstein. 2011. MDAnalysis: A toolkit for the analysis of molecular dynamics simulations. J. Comput. Chem. 32: 2319–2327.
32. 2018. Spyder: The Scientific Python Development Environment. .
33. Sethi, A., J. Eargle, A.A. Black, and Z. Luthey-Schulten. 2009. Dynamical networks in tRNA: Protein complexes. Proc. Natl. Acad. Sci. U. S. A. 106: 6620–6625.
34. Eargle, J., and Z. Luthey-Schulten. 2012. Network view: 3D display and analysis of protein ·rNA interaction networks. Bioinformatics. 28: 3000–3001.
35. Humphrey, W., A. Dalke, and K. Schulten. 1996. VMD: Visual molecular dynamics. J. Mol. Graph. 14: 33–38.
36. Girvan, M., and M.E.J. Newman. 2002. Community structure in social and biological networks. Proc. Natl. Acad. Sci. U. S. A. 99: 7821–7826.
37. Bayburt, T.H., Y. V. Grinkova, and S.G. Sligar. 2002. Self-Assembly of Discoidal Phospholipid Bilayer Nanoparticles with Membrane Scaffold Proteins. Nano Lett. 2: 853–856.